Evaluation and comparison of CanRCM4 and CRCM5 to estimate probable maximum precipitation over North America

Mohamed Ali Ben Alaya, Francis W. Zwiers, & Xuebin Zhang

2019

Original citation:

Ben Alaya, M. A., Zwiers, F. W., & Zhang, X. (2019). Evaluation and comparison of CanRCM4 and CRCM5 to estimate probable maximum precipitation over North America. *Journal of Hydrometeorology*, *20*(10), 2069–2089. https://doi.org/10.1175/JHM-D-18-0233

Evaluation and Comparison of CanRCM4 and CRCM5 to Estimate Probable Maximum Precipitation over North America

M. A. BEN ALAYA AND F. ZWIERS

Pacific Climate Impacts Consortium, University of Victoria, Victoria, British Columbia, Canada

X. ZHANG

Climate Research Division, Environment and Climate Change Canada, Toronto, Ontario, Canada

(Manuscript received 29 October 2018, in final form 15 July 2019)

ABSTRACT

Recently dam managers have begun to use data produced by regional climate models to estimate how probable maximum precipitation (PMP) might evolve in the future. Before accomplishing such a task, it is essential to assess PMP estimates derived from regional climate models (RCMs). In the current study PMP over North America estimated from two Canadian RCMs, CanRCM4 and CRCM5, is compared with estimates derived from three reanalysis products: ERA-Interim, NARR, and CFSR. An additional hybrid dataset (MSWEP-ERA) produced by combining precipitation from the Multi-Source Weighted-Ensemble Precipitation (MSWEP) dataset and precipitable water (PW) from ERA-Interim is also considered to derive PMP estimates that can serve as a reference. A recently developed approach using a statistical bivariate extreme values distribution is used to provide a probabilistic description of the PMP estimates using the moisture maximization method. Such a probabilistic description naturally allows an assessment of PMP estimates that includes quantification of their uncertainty. While PMP estimates based on the two RCMs exhibit spatial patterns similar to those of MSWEP-ERA and the three sets of reanalyses on the continental scale over North America, CanRCM4 has a tendency for overestimation while CRCM5 has a tendency for modest underestimation. Generally, CRCM5 shows good agreement with ERA-Interim, while CanRCM4 is more comparable to CFSR. Overall, the good ability of the two RCMs to reproduce the major characteristics of the different components involved in the estimation of PMP suggests that they may be useful tools for PMP estimation that could serve as a basis for flood studies at the basin scale.

1. Introduction

Probable maximum precipitation (PMP) is the greatest accumulation of precipitation for a given duration meteorologically possible for a given area at a particular time of year, with no allowance made for long-term climatic trends (WMO 2009). PMP is required to estimate the largest flood that could occur in a given watershed, known as the probable maximum flood (PMF). The PMP/PMF is a rational engineering concept used to provide informational products commonly needed for the design of infrastructure for water retention (dams), where failure would be disastrous (Kunkel et al. 2013).

Operational PMP estimation procedures, which involve a number of steps, assumptions, data that are uncertain, and physical judgments, seek to obtain estimates of precipitation amounts that are unlikely to be exceeded. An approach that is often used by engineers is the so-called moisture maximization method. Moisture maximization (WMO 2009) considers that a storm has two relevant factors: precipitable water (PW) and precipitation efficiency (PE) (Rakhecha and Clark 1999). PW is the total atmospheric column water vapor, whereas PE is the ratio of the actual precipitation amount to PW. The moisture maximization approach obtains PMP estimates as the product of the maximum PE of

Denotes content that is immediately available upon publication as open access.

Supplemental information related to this paper is available at the Journals Online website: https://doi.org/10.1175/JHM-D-18-0233.s1.

Corresponding author: M. A. Ben Alaya, mohamedalibenalaya@uvic.ca

DOI: 10.1175/JHM-D-18-0233.1

historically important storms with the climatologically maximum PW.

Global climate models (GCMs) are useful for simulating the large-scale climate evolution and to develop and examine projected changes in climate extremes and especially extreme precipitation events at the scales that are resolved by the models. However, information provided by GCMs cannot be directly used by many users of climate information due to their coarse resolution. Regional climate models (RCMs) have been developed to downscale GCMs to a higher resolution, and thus to provide information at regional scales that is better suited to basin representation for hydrological studies.

In the context of climate change and the projected increase in global temperature, the atmosphere's water holding capacity is expected to increase by about 7% per 1°C warming according to the Clausius–Clapeyron equation. Global temperature is projected to increase by 2.6°–4.8°C by the late twenty-first century over its 1986–2005 value under the RCP8.5 scenario (Collins et al. 2013). Such increases may lead to more intense precipitation events. Hence, updating PMP estimates to consider future climate conditions represents a growing issue that needs to be addressed for dam safety. In this regard, the direct use of RCM simulations may provide a straightforward and comprehensive way to derive PMP estimates corresponding to future climate conditions. Although RCMs and climate models have started to be used to derive PMP estimates in the last few years (Ohara et al. 2011; Beauchamp et al. 2013; Rousseau et al. 2014; Rouhani and Leconte 2016; Chen et al. 2017; Rastogi et al. 2017; Chen and Hossain 2018; Gangrade et al. 2018; Yang and Smith 2018), a careful evaluation of their performance with respect to PMP estimation as well as the different components involved in calculating PMP is required. For instance, Paquin et al. (2016) showed that PW from version 4.2.4 of the Canadian Regional Climate Model (CRCM) could be incorporated into PMP and PMF studies and suggest that this might hold for RCMs in general.

While it is important to assess PMP calculated from RCM outputs, increasing the confidence in the reliability of such assessments remains a big challenge due to the deterministic nature of most PMP estimation methods. Indeed, PMP estimation methods generally produce only single values that are not accompanied by uncertainty estimates. The fact that uncertainty is not quantified for PMP estimates has been criticized by many hydrologists (Benson 1973; Kite 1988; Koutsoyiannis 1999; Papalexiou and Koutsoyiannis 2006; Dingman 2008; Shaw et al. 2010; Salas et al. 2014; Micovic et al. 2015; Chen et al. 2017). Nevertheless, only few studies have considered the uncertainty of PMP estimates (Salas et al. 2014; Micovic et al. 2015; Salas and Salas 2016).

The main objective of this paper is to compare and assess PMP estimates based on the output of two Canadian regional climate models, CanRCM4 and CRCM5, over North America. To this end, a probabilistic extension of the usual moisture maximization method proposed by Ben Alaya et al. (2018) is adopted to provide a probabilistic description of the operational PMP estimate obtained using the moisture maximization method. Such a probabilistic description naturally leads to an assessment of the ability of the two RCMs to support PMP estimation that includes quantification of their uncertainties. This approach uses a bivariate extreme value model based on asymptotic theory to approximate the joint distribution of the annual extremes of PE and PW. A copula function is used to represent the dependence between PW and PE extremes. The remainder of the paper is structured as follows. The next section describes the datasets and methods. Results and discussions are given in section 3, followed by conclusions that are given in section 4.

2. Datasets and methods

a. Datasets

Our study compares and assesses the ability of the two recently developed Canadian RCMs, CanRCM4 and CRCM5, to support PMP estimation over North America. Model simulations were assessed over the period 1979–2005. CRCM5 (Hernández-Díaz et al. 2013; Laprise et al. 2013; Šeparović et al. 2013) was developed by the Centre pour l'Étude et la Simulation du Climat à l'Échelle Régionale (ESCER) at UQAM, whereas CanRCM4 (Scinocca et al. 2016) was developed by the Canadian Centre for Climate Modelling and Analysis (CCCma) at Environment and Climate Change Canada. Both models are used in the international Coordinated Regional Climate Downscaling Experiment (CORDEX; Giorgi et al. 2009) project. They share the same dynamics as Environment Canada's Global Environmental Multiscale (GEM) forecast model (Côté et al. 1998) but use different packages of physical parameterizations. Both RCMs use a rotated pole grid (83.0°W and 42.5°N). Multiple CanRCM4 and CRCM5 runs driven by the second generation Canadian Earth System Model (CanESM2) are available for both historical and future climates. Most of the available CanRCM4 runs use spectral nudging for scales larger than 1000 km, while most CRCM5 runs have a free interior. In this work we focus mainly on one run for each of CanRCM4 and CRCM5, where both runs are driven by the same CanESM2 simulation. Both runs are at a horizontal resolution of 0.44°. The CanRCM4 run uses spectral nudging while the CRCM5 run is free (see Table 1 for

TABLE 1. Details about regional climate models used in the current analysis.

	Institute	Boundary condition	Spatial resolution (°)	Domain size	Interior
CanRCM4	CCCma	CanESM2	0.44	155 × 130	Spectral nudging
CRCM5	UQAM	CanESM2	0.44	172 × 160	Free

descriptions of the RCM simulations). From the numerous variables that are available from these models, we used the total precipitation and precipitable water (corresponding the water vapor path vertically integrated through the atmospheric column), both at a 6-hourly temporal resolution.

The decision to analyze CanESM2 driven simulations implies that some biases in outputs of the RCMs may be due to biases that are propagated from the driving CanESM2 run. While this bias component might be avoided by using reference simulations that are driven by ERA-Interim, such simulations are only available from 1989 to 2009, which is too short to reliably fit the bivariate extreme value model. In addition, our main interest is to evaluate historical RCM runs that will subsequently be used to provide reference levels for projecting future changes in PMP.

The model simulations will be compared to three reanalysis products over the period 1979–2005: the North American Regional Reanalysis (NARR; 0.33°) (Mesinger et al. 2006), ERA-Interim (0.75°) (Dee et al. 2011), and the NCEP Climate Forecast System Reanalysis (CFSR; 0.31°) (Saha et al. 2010). The main advantage of using reanalyses is that their gridded output is more comparable to model output representing spatial scales of a gridbox size and larger, as opposed to station data that are by their nature local point measurements. A researcher using the reanalysis for comparison should be aware, however, that the different outputs of reanalysis products are not uniformly reliable. The precipitable water is partially defined by the observations but is also strongly influenced by the model characteristics, which is why it is classified as a type B (although there are observational data that directly affect the value of the variable, the model also has a very strong influence on the analysis value) variable in Kalnay et al. (1996). Confidence in precipitation from reanalyses is generally much lower than that in precipitable water because precipitation observations are generally not assimilated, and thus precipitation would typically be considered to be a type C (indicating that there are no observations directly affecting the variable, so that it is derived solely from the model fields forced by the data assimilation to remain close to the atmosphere) variable. In general, precipitation from reanalyses is only weakly constrained in the model by assimilated observations. An exception is the NARR, which does assimilate precipitation observations to adjust the accumulated convective and gridscale precipitation, the latent heating, the moisture, and the cloud fields based on differences between the modeled and observed hourly precipitation. While the NARR precipitation assimilation scheme ensures a somewhat more realistic representation of precipitation, the reliability of the NARR product is not spatially uniform and is strongly related to the rain-gauged density. For instance, Mo et al. (2005) and Mesinger et al. (2006) identify that NARR precipitation products are less reliable outside the United States where fewer observations are assimilated. Given all these issues with using precipitation from reanalysis, an additional precipitation dataset, the Multi-Source Weighted-Ensemble Precipitation (MSWEP) dataset (Beck et al. 2017) over the period 1979–2005, is also considered. MSWEP merges surface-based observations, remotely sensed observations, and reanalysis products to create a global 3-hourly precipitation dataset on a 0.25° grid that is specifically designed for hydrological modeling. The long-term mean of precipitation in MSWEP is based on the CHPclim dataset, but is replaced with more accurate regional datasets where available. In addition a correction for gauge undercatch and orographic effects is performed in MSWEP by inferring catchment-average precipitation from streamflow observations at 13 762 stations across the globe. The temporal variability of precipitation is determined by weighted averaging of precipitation anomalies from seven datasets including rain gauge measurements (CPC Unified and GPCC), three satellite remote sensing products (CMORPH, GSMaP-MVK, and TMPA 3B42RT), and two atmospheric model reanalyses (ERA-Interim and JRA-55). Details, including references for the datasets that are incorporated in the MSWEP product, can be found in Beck et al. (2017).

We use precipitation data from MSWEP together with PW data from ERA-Interim to construct a PE dataset that can serve as a reference for the comparison between RCMs and reanalysis products. A bivariate extreme value model combining precipitation from MSWEP and PW from ERA-Interim will also be used to compute PMP values that can serve as reference for comparison and assessment purposes.

b. Methods

Moisture maximization is the commonly used approach to estimate PMP. This approach involves a

computation that separately maximizes PW and PE and considers the PMP event as the worst case scenario under which the maximum PE and maximum PW events occur simultaneously. Hence, operationally, PMP would be obtained as the product of the two maximums. However moisture maximization suffers from inherent drawbacks related to (i) the sensitivity of the PMP value to two particular observations, the maximum observed PW over the entire PW sample, and the maximum PE for the entire PE sample; (ii) the lack of consideration of a realistic dependence structure between PE and PW extremes due to the assumption of the simultaneous occurrence of the two maxima; and finally (iii) the fact that the uncertainty of the calculated PMP value is not quantified. To address these drawbacks, Ben Alaya et al. (2018) proposed a bivariate extreme value analysis model to produce PMP estimates and quantify their uncertainty. This approach, which is used in the current analysis, is based on simulating PMP values using a bivariate extreme value model of PE and PW. The model is briefly described in the following section 2b(1), while the algorithm for deriving PMP estimates as well the comparison and assessment method are presented in the following section 2b(2).

1) Bivariate extreme value analysis of extreme PW and PE

In a first step, the generalized extreme value (GEV) distribution is used to approximate the marginal distributions of the seasonal maxima of PW and PE. The GEV distribution is given by

$$G(y;\mu,\sigma,\xi)=\begin{cases}\exp\left\{-\left[1+\xi\left(\dfrac{y-\mu}{\sigma}\right)\right]^{-1/\xi}\right\}, & \text{if} \quad \xi\neq 0,\\ \exp\left[-\exp\left(-\dfrac{y-\mu}{\sigma}\right)\right], & \text{if} \quad \xi=0,\end{cases} \tag{1}$$

which is defined on $\{y{:}1+\xi(y-\mu)/\sigma>0\}$. The location parameter ($-\infty<\mu<\infty$) determines the position of the PDF, and the scale parameter ($\sigma>0$) determines the width of the PDF. The shape parameter ($-\infty<\xi<\infty$) describes the form of the decay of the distribution in the upper tail, that is, for large values of y (Coles et al. 2001; Embrechts et al. 2013). We fit GEV distributions separately to maxima of PW and PE for each grid box and for each season. The three GEV distribution parameters are estimated using the robust method of L-moments (Hosking 1990). The shape parameter is subsequently adjusted to ensure feasibility as suggested by Dupuis and Tsao (1998).

The joint behavior of the PE and PW extremes, including their dependence, can be considered by using an extreme value copula function to connect the two GEV distributions. Sklar's theorem states that every joint cumulative distribution function $H(x, y)$ of the random variables X and Y can be expressed in terms of its margins $F(x)$ and $G(y)$ and a copula function C as

$$H(x,y)=C\{F(x),G(y)\},x,y\in\mathbb{R}, \tag{2}$$

where $C{:}I\times I\rightarrow I(I=[0,1])$ such that

1) for every $u,v\in I$, $C(u,0)=0$, $C(u,1)=u$, $C(0,v)=0$ and $C(1,v)=v$, and
2) for every $u_1,u_2,v_1,v_2\in I$ where $u_1\leq u_2$ and $v_1\leq v_2$, $C(u_2,v_2)-C(u_2,v_2)-C(u_2,v_1)-C(u_1,v_2)+C(u_1,v_1)\geq 0$.

An extreme value copula C has the further property of being max stable, meaning that if (U_1, V_1), (U_2, V_2), ..., (U_n, V_n) are independent and identically distributed (iid) random pairs from C and $P_n=\max\{U_1, U_2,..., U_n\}$ and $Q_n=\max\{V_1, V_2, ..., V_n\}$, then the copula associated with the random pair (P_n, Q_n) is also C (Beirlant et al. 2006; Genest and Segers 2009). Any extreme value copula may be expressed in the following form (Genest and Segers 2009):

$$C(u,v)=(uv)^{A[\log(u)/\log(uv)]},(u,v)\in[0,1]^2, \tag{3}$$

where $A{:}[0,1]\rightarrow[1/2,1]$ is convex and satisfies $\max\{1-t,t\}\leq A(t)\leq 1\ \forall\ t\in[0,1]$. The term A is known as the Pickands dependence function. As in Ben Alaya et al. (2018), we use the Gumbel copula in the current work due to its ease of implementation and the ease of simulation from the Gumbel copula. The Gumbel copula with parameter θ is an extreme value copula with dependence function $A(s)=[s^\theta+(1-s)^\theta]^{1/\theta}$. We estimate θ using the maximum likelihood method. While there are many parametric copula models, we are limited to the use of an extreme value copula. In addition, the Gumbel copula is the only extreme value copula that is also Archimedean (which have the benefit of being well studied in the statistical literature, indeed many well-known systems of bivariate distributions belong to this class) (Genest and Rivest 1993). Previous studies as discussed in Ben Alaya et al. (2018) have demonstrated that the Gumbel copula performs well for modeling multivariate hydrological extremes (Serinaldi 2008). One approach that can be used to assess the suitability of the Gumbel copula is to compare the upper tail dependence coefficient estimates obtained by fitting the Gumbel copula to the corresponding nonparametric estimator of Capéraà et al. (1997). This coefficient describes the dependence between extreme values of PW and PE. Ben Alaya et al. (2018) demonstrate that

the Gumbel copula performs well in representing the tail dependence of CanRCM4 simulated seasonal and annual PW and PE extremes.

2) PMP USING THE BIVARIATE EXTREME VALUE MODEL

To estimate a PMP value at a given location, the bivariate GEV models that were fitted for each season at that location can be used to simulate seasonal maxima of PE and PW and thus to obtain an annual maximized precipitation value for each grid box (Ben Alaya et al. 2018). A simulated PMP value based on an m-year record can then be obtained by keeping the largest of m simulated annual maximized precipitation amounts. Repeating this process a number of times allows us to simulate the distribution of PMP based on m-year records, and thus its uncertainty.

We apply the simulation approach using estimates of seasonal bivariate extreme value distributions of PE and PW that are based on data covering a short 27-yr period (the length of the shortest reanalysis). Nevertheless, the PMP distribution is obtained by simulating periods of length $m = 100$ years from the fitted bivariate distributions. The choice of $m = 100$ years is arbitrary, although WMO (2009) does recommend that a 100-yr return level for PW be considered as the climatological maximum PW when estimating PMP from data records shorter than 50 years. The small sample size that is used to fit the bivariate extreme value distribution implies that the derived PMP estimates may be affected by high uncertainty. We therefore also incorporate simulation steps that account for this source of sampling uncertainty. The following algorithm is therefore used for each grid box (Ben Alaya et al. 2018) to simulate a distribution for PMP based on years that also accounts for uncertainty in the fitting of the bivariate extreme value model for PE and PW:

1) Draw four random samples of 27 pairs of PE and PW seasonal maxima (one sample of 27 pairs for each season) with replacement from available data. The resampling is done on years such that selecting a year implies that all bivariate seasonal maxima for that year have the corresponding data value included in the bootstrap samples.
2) Fit the four bivariate extreme value models to each of the four samples drawn in step 1 so that one bivariate GEV model is available for each season.
3) Draw a sample of $m = 100$ independent pairs of PE and PW extremes from each of the four bivariate distributions obtained in step 2.
4) Compute the products of the simulated $4 \times m$ pairs of extreme PE and PW values drawn in step 3.
5) Keep the largest of the products computed in step 4; this value represents one realization of PMP estimated via moisture maximization based on an m-year sample. The use of four bivariate GEV models corresponding to each season ensures that the simulated PMP value is obtained using PW and PE values occurring within the same season, as it is commonly recommended in practice.
6) Repeat steps 1–5 to simulate the expected variation in PMP estimates that would occur in repeated analyses of independent m-year periods under the same hydroclimatic conditions.

This algorithm uses a doubly nested resampling strategy. In a first step, regular nonparametric resampling with replacement (simple bootstrap sampling) accounts for sampling error in the estimated bivariate GEV model, while the second step (parametric resampling) allows simulation of a PMP value and accounts for sampling error in that value given the fitted bivariate GEV distribution. Leaving aside the uncertainties that are due to the different steps involved in PMP estimation (Micovic et al. 2015), as well uncertainties due to the choice of data source (selection of one many possible GCMs or reanalyses) for driving the RCM, the two resampling operations, in sequence, allow us to quantify the combined impact of the two sources of sampling error regarding the input data.

A number of multivariate statistical models are available to represent the dependence between extremes. The bivariate extreme value model used here is obtained as an extension of the univariate GEV model. Depending on the choice of the extreme value copula that is incorporated into the bivariate model, PMP estimates will either reproduce the operational moisture maximization calculation or differ somewhat from that calculation (Ben Alaya et al. 2018). The proposed approach will nevertheless provide uncertainty estimates in both cases. It should be noted that the bivariate extreme value model is based on asymptotic theory whereby the two components, PW and PE, converge to their limiting distributions at the same rate. Application of the theory requires a decision about whether are PW and PE independent or dependent in the asymptotic limit. Ben Alaya et al. (2018) show that the traditional operational approach requires the assumption of total dependence between the annual extremes of PE and PW, which may lead to an overmaximization in PMP estimates. While we still assume asymptotic dependence, the total dependence assumption is relaxed by modeling seasonal extremes using an extreme value copula that can represent different degrees of dependence.

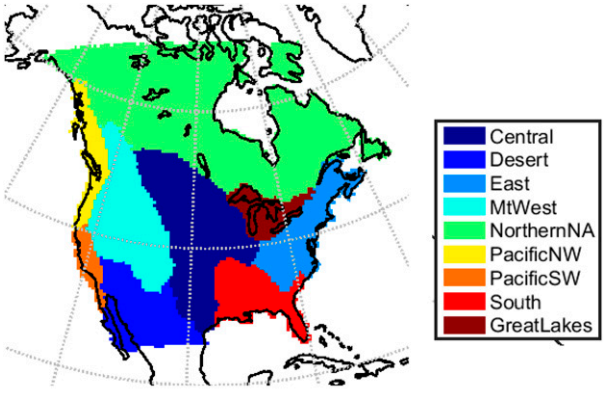

FIG. 1. Bukovsky regions used in this study over North America.

3) COMPARISON AND ASSESSMENT METHOD TO DERIVE PMP ESTIMATES

To assess PMP estimates over North America derived from the outputs from the two RCMs, we fit bivariate extreme values distributions to seasonal maxima of PW and PE for both RCMs, the three sets of reanalyses, and the MSWEP-ERA dataset. Grid cells representing the ocean on the native grid of each dataset were removed. To simplify subsequent data manipulation the seasonal maxima from the reanalyses, MSWEP-ERA and CRCM5 were interpolated to correspond to the CanRCM4 CORDEX North America grid using the k nearest neighbor method.

A common approach for computing PMP often involves the use of storm transposition (Foufoula-Georgiou 1989) as a means of incorporating additional information about precipitation events from nearby locations. Ben Alaya et al. (2018) exploited the gridded nature of climate model output to incorporate a simplified transposition step pooling the block maxima of precipitation efficiency using 3×3 moving windows of grid boxes. In the same way, in the current work we separately fit the seasonal GEV distributions to maxima of seasonal maxima of PE from the surrounding 3×3 grid box region (only the maximum surrounding 3×3 grid box region is retained for each year) and to the seasonal maxima of PW at the grid box.

Once distributions are fitted, we first assess how well the RCMs reproduce the three components of the bivariate extreme value distribution (the marginal GEV distributions for PE and PW and the Gumbel copula) for each season at each grid box over North America. Following this, the two PMP estimates that are obtained for each RCM are assessed at grid boxes. The models are also assessed at the scale of the Bukovsky regions (Bukovsky 2012) presented in Fig. 1. For the latter, regional bivariate extreme value distributions were obtained by spatially averaging the bivariate GEV model parameters obtained in step 2 of the resampling process for each Bukovsky region. Then, regional PMP estimates were obtained by using the resulting regional bivariate distribution in each step 3 of the simulation algorithm. Again, the two RCMs were assessed and compared to reanalyses and MSWEP-ERA, first, based on their abilities to reproduce the three components of each regional bivariate extreme value distribution for each season, and then based on their abilities to derive regional PMP estimates. This regionalization is used to provide a summary of findings for a "typical" 3×3 gridbox area within a given Bukovsky region. This is justified by the fact that Bukovsky regions reflect, at a large scale, roughly consistent temperature, precipitation and storm track climatologies. The characterization of typical PMP estimates within Bukovsky regions should not be confused with regionalization steps (such as storm transposition) that are commonly used to reduce uncertainty in model parameter estimates by pooling information within homogenous regions.

3. Results and discussions

a. *Precipitable water results*

Univariate GEV models are first fitted separately to the seasonal maxima of PE from the surrounding 3×3 grid box region and to the seasonal maxima PW at the grid box for the two RCMs and the three reanalyses. The Kolmogorov–Smirnov (KS) goodness-of-fit test is used at each grid box to assess the differences between the empirical and the fitted GEV cumulative distributions at the 5% significance level. Note however, that the small 27-yr sample size will considerably restrict the power of this test to detect lack of fit. Figure 2 presents maps of the estimated GEV parameters of PW winter maxima for the two RCMs and the three sets of reanalyses, plotted on the CanRCM4 grid. KS test results are also shown in Fig. 2. Similar figures for each of the other seasons are presented in the online supplemental material (see Figs. S1–S3). In the case of PW, the KS tests indicate that a GEV distribution reasonably approximates the distribution of extremes of PW over the majority of grid boxes of both RCMs and reanalysis products for the winter season (DJF). The percentage of grid boxes failing the KS test is equal to 0.8% in CanRCM4 and CRCM5, 2.9% in ERA-Interim, 5.2% in NARR, and 4.5% in CFSR during the winter, and comparable results were obtained for the other seasons. Most of the grid boxes failing the KS test are located in areas of complex topography, along the west coast of the continent and in the Mountain West (MtWest) region.

As shown in Fig. 2 and similar figures for other seasons in the supplemental material (Figs. S1–S3), there is very good agreement between the GEV parameters in all

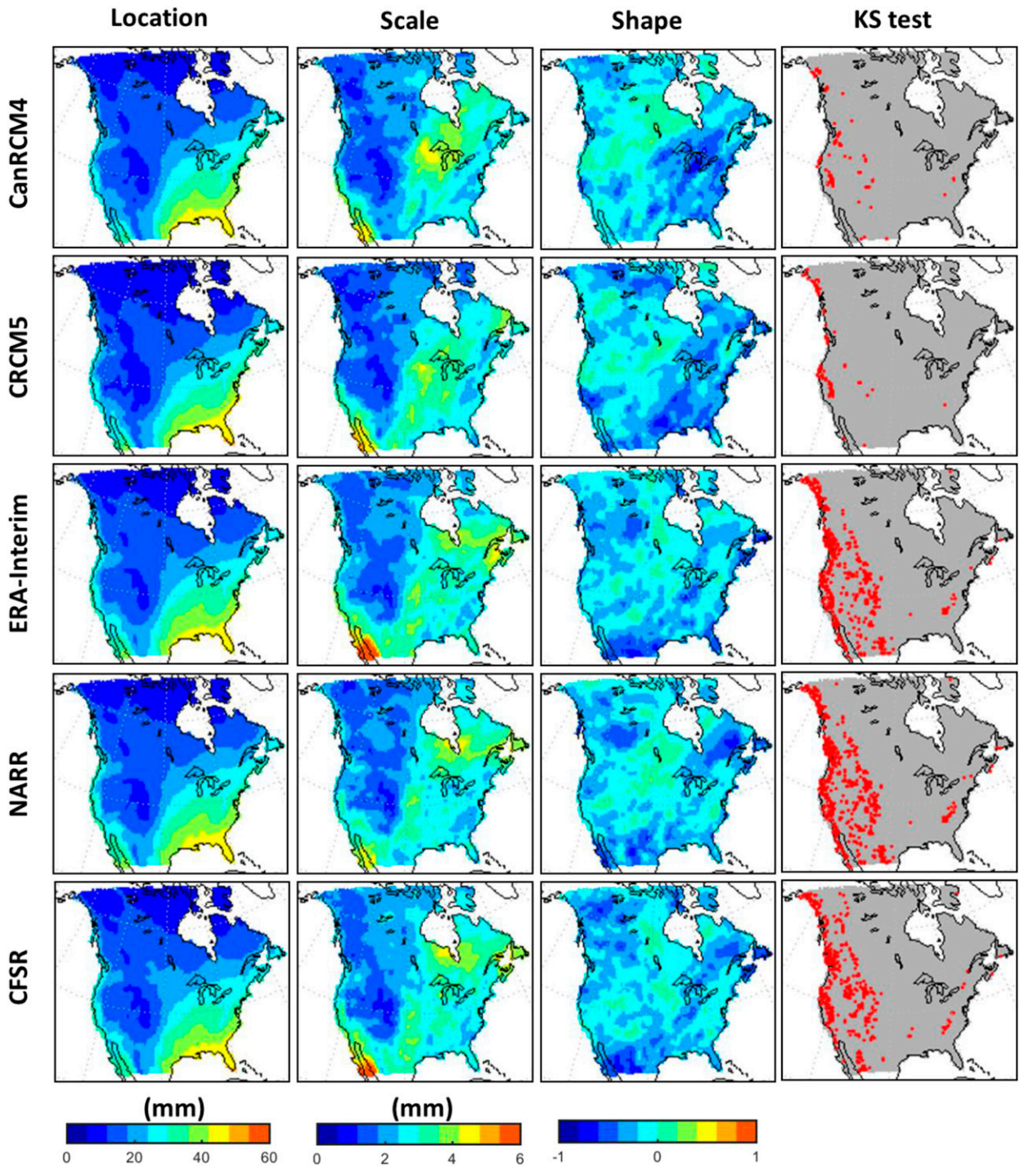

FIG. 2. Estimated GEV model parameters for PW for both RCMs and reanalyses for the winter season (DJF). Red points in the KS test column denote locations of grid boxes failing the KS test.

models mainly for the location parameters where some common features are obvious in both RCMs and reanalysis for all seasons. These include high values over Baja California, reduced values over the Appalachians, and a visible dryline in central North America that separates the moist air from the Gulf of Mexico and the dry air from the desert southwestern states. High values of the scale parameter can be seen over Baja California in both RCMs and reanalyses for all seasons except the summer. Note that CanRCM4, with broadly larger scale

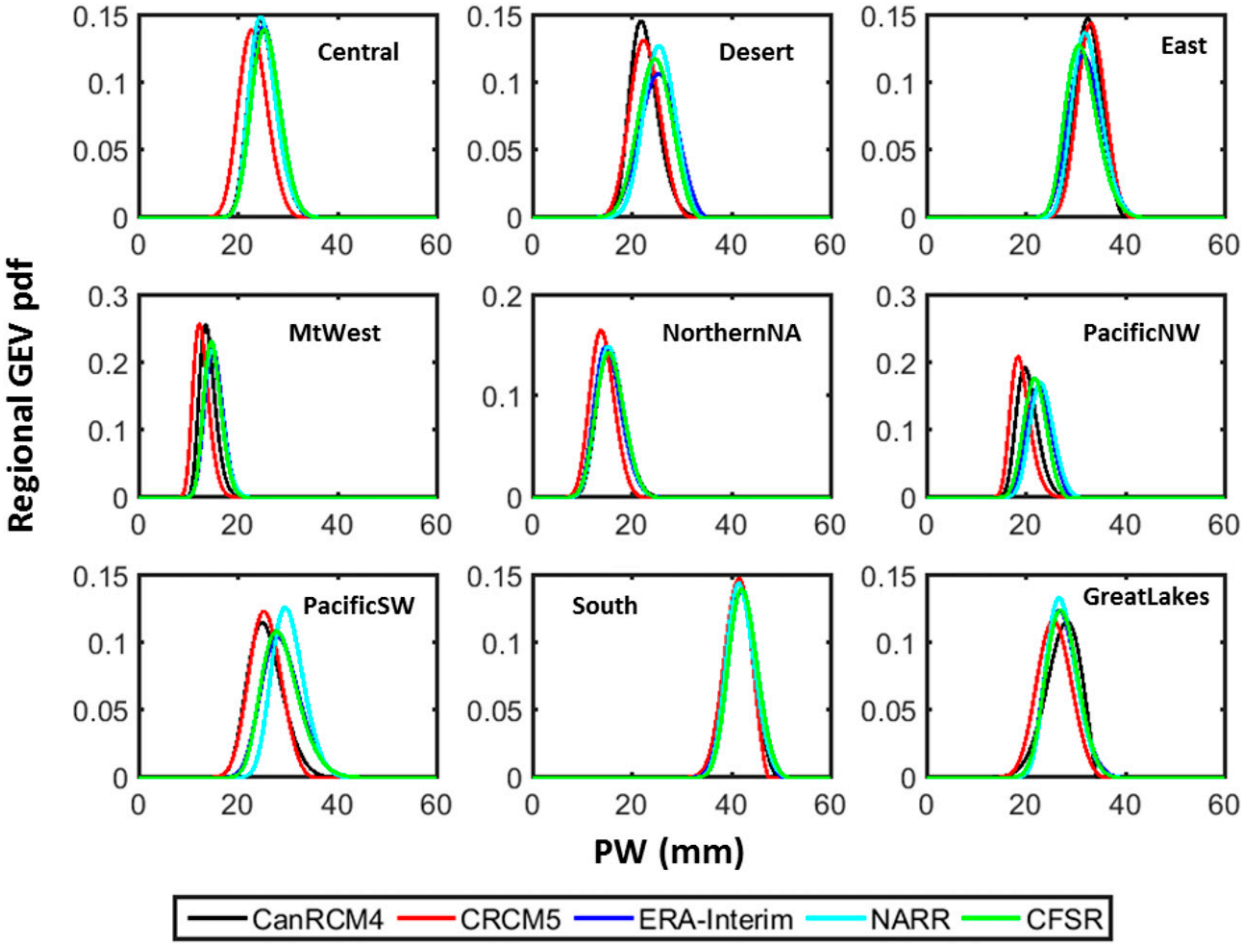

FIG. 3. PDF plots of the regional precipitable water GEV distribution for both RCMs and reanalyses during DJF.

parameter values east of the dryline during the summer season, appears to be a bit different compared to CRCM5 and the reanalyses. On the other hand, while the seasonal scale parameter estimates are noisy, there is broad consensus between models and reanalyses on average. With a frequently near zero, or negative shape parameter estimates, the two Canadian RCMs show good general agreement with the reanalyses in reproducing the shape parameter. In conclusion empirical evidence from both the RCMs and reanalyses suggests that PW is bounded. While the noisy shape parameter estimates are harder to interpret, two prominent dissimilarities between RCMs and reanalysis are apparent. The first is the positive values in the RCMs over the western part of North America that are not seen in the reanalyses. The second is the positive values over the southeast in reanalysis that are not seen in the RCMs during the fall and winter seasons. Both of these differences could be related to driving the RCMs with CanESM2 rather than reanalyses.

Precipitable water GEV distributions representative of locations within Bukovsky regions are obtained by averaging single grid boxes GEV parameters over each Bukovsky region. As shown in Fig. 3, on the continental scale, the PDFs of PW for both RCMs are in good agreement with reanalyses during the winter. Similar figures to Fig. 3 for the other seasons are presented in supporting information (see Figs. S4–S6). For the other season, where there are differences, CRCM5 tends to outperform CanRCM4 and exhibits better agreement with reanalysis products. During the fall and summer, the CanRCM4 PDF is shifted to lower values compared to the other PDFs, mainly in the Central, Desert, PacificSW, and South regions, and hence exhibits a negative bias compared to reanalysis products.

b. Precipitation efficiency results

We now evaluate the ability of the two RCMs to adequately reproduce the distribution of seasonal maxima of PE. The percentage of grid boxes failing the KS test performed at the 5% significance level is smaller than or consistent with the expected 5%, with values between 0.8% in ERA-Interim during the spring (see Fig. S7) and

8% in NARR during the winter (see Fig. 4). Similar to PW, grid boxes where the KS test fails are mostly located along the west coast of the continent and in the Mountain West region. Particularly, for NARR, grid boxes failing the KS test were also found along the U.S. borders during the spring and summer seasons (see Figs. S7 and S8). This is presumably related to the use of different precipitation data sources from different countries in the precipitation assimilation process. In general, we may conclude that there is little evidence of an obvious misfit of the GEV distribution to annual maximum PE in both RCMs and reanalyses in most regions.

Maps of the estimated GEV parameters of PE winter maxima for the two RCMs and reanalyses are presented in Fig. 4. GEV parameters of PE for the other seasons are also shown in the supplemental material (Figs. S7–S9). Extreme PE distributions appear to be less consistent between models than for PW. There is substantial dissimilarity between the reanalyses as well, and thus direct comparison of the two RCMs with the reanalyses in term of PE does not allow us to draw conclusions about which model performs better than the other. Indeed the reliability of reanalyses to produce PE also needs to be assessed. To this end, MSWEP-ERA data that is constructed by combining precipitation data from MSWEP with PW data from ERA-Interim is used as a reference. The choice of ERA-Interim reanalysis, here, among reanalysis, is arbitrary; it is expected that this choice does not influence the constructed data due to the high level of similarity between PW simulated from the three reanalyses. Maps of estimated GEV parameters of PE annual maxima for MSWEP-ERA data are also presented in Fig. 4 (as well in corresponding figures in the supplemental material). As one can note, the shape parameter of seasonal maxima of PE does not exhibit strong spatial variation for any of the datasets. In contrast to annual maximum PW, which is dominantly Weibull, annual maximum PE is most frequently Gumbel. Indeed the mean value of the shape parameters over all North America is approximately zero (see Fig. 4). Exceptions are the PacificSW region during the summer and the Desert region during the spring and summer, where all models show that PE maxima seem to be dominantly Weibull. In conclusion, empirical evidence through the extreme value theory suggests that PW is bounded whereas PE is unbounded. We suspect that such a result may reflect the role of atmospheric convergence in transporting moisture into the atmospheric column, thereby replenishing moisture that precipitates out of the atmospheric column. Such a process can, over a 6- or 24-h period, result in accumulations several times larger than PW.

The lack of consistency in reproducing extreme PE in both RCMs and reanalyses can be in part linked to their dissimilarity in reproducing extreme precipitation [see Fig. S10; also a basic assessment of CanRCM4 and CRCM5 abilities to simulate precipitation extremes can be found in Whan and Zwiers (2016)]. Since CanRCM4 and CRCM5 share the same dynamical core and are driven by the same CanESM2 simulations, the dissimilarity between them would be mainly related to their physics packages and possibly their driving strategies (i.e., whether spectral nudging is used). By examining the GEV parameters of PE annual maxima obtained from a CanRCM4 simulation without spectral nudging (not shown) we did not find a significant difference with the CanRCM4 spectrally nudged simulation analyzed in this study. Hence, we conclude that the driving strategy is not likely the main cause of the dissimilarity between the two RCMs. Instead, this is more likely due to differences in their physical packages including the differences in the parameterization of convective and stratiform precipitation (Scinocca et al. 2016).

On the continental scale both RCMs and reanalyses exhibit reasonable spatial correlation with MSWEP-ERA (see Fig. 5) data for the location parameter and in some cases the scale parameter of seasonal extreme PE. Whereas for the shape parameter, this spatial correlation is lower for both RCMs and reanalyses, with CFSR exhibiting the highest correlation for all seasons. Such small correlations related to the shape parameter estimates are expected. Indeed these small correlations reflect the high uncertainty in the shape parameter estimates and the possibility that there may be little real spatial variation in their values. In terms of root-mean-square differences (RMSD), CRCM5 performs somewhat better than CanRCM4 for the three parameters during the spring and summer seasons (see Figs. S7 and S8).

Regional GEV distributions for PE were obtained by averaging gridbox GEV parameters over each Bukovsky region. As shown in Fig. 6 and Figs. S11–S13, in most regions, and most seasons CanRCM4 is more comparable, in general, to ERA-Interim and CFSR. CRCM5 PDF is shifted to higher values compared to the other PDFs during the winter and fall seasons and hence exhibits positive biases compared to reanalysis products and MSWEP-ERA. On the other hand, NARR generally exhibits positive biases compared to the other models over most regions and seasons. As we can see from Fig. 7, CRCM5, in general, underestimates the PE shape parameter for most regions and seasons compared to the other models. This result may offset the positive biases exhibited during the winter and fall seasons in simulating extreme precipitation events. The largest negative biases

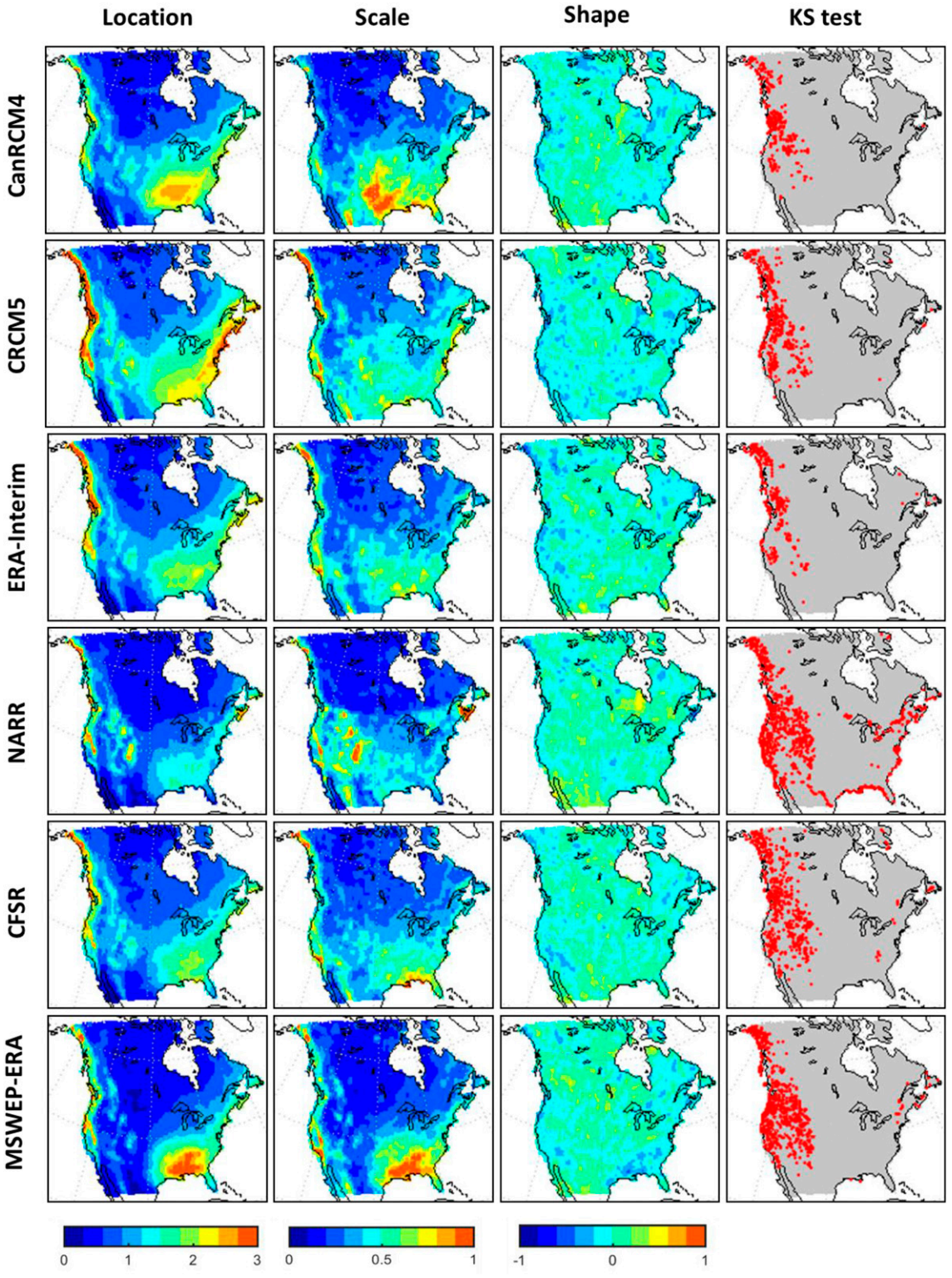

FIG. 4. Estimated GEV model parameters for PE for both RCMs, reanalyses, and MSWEP-ERA for DJF. Red points in the KS test column denote locations of grid boxes failing the KS test.

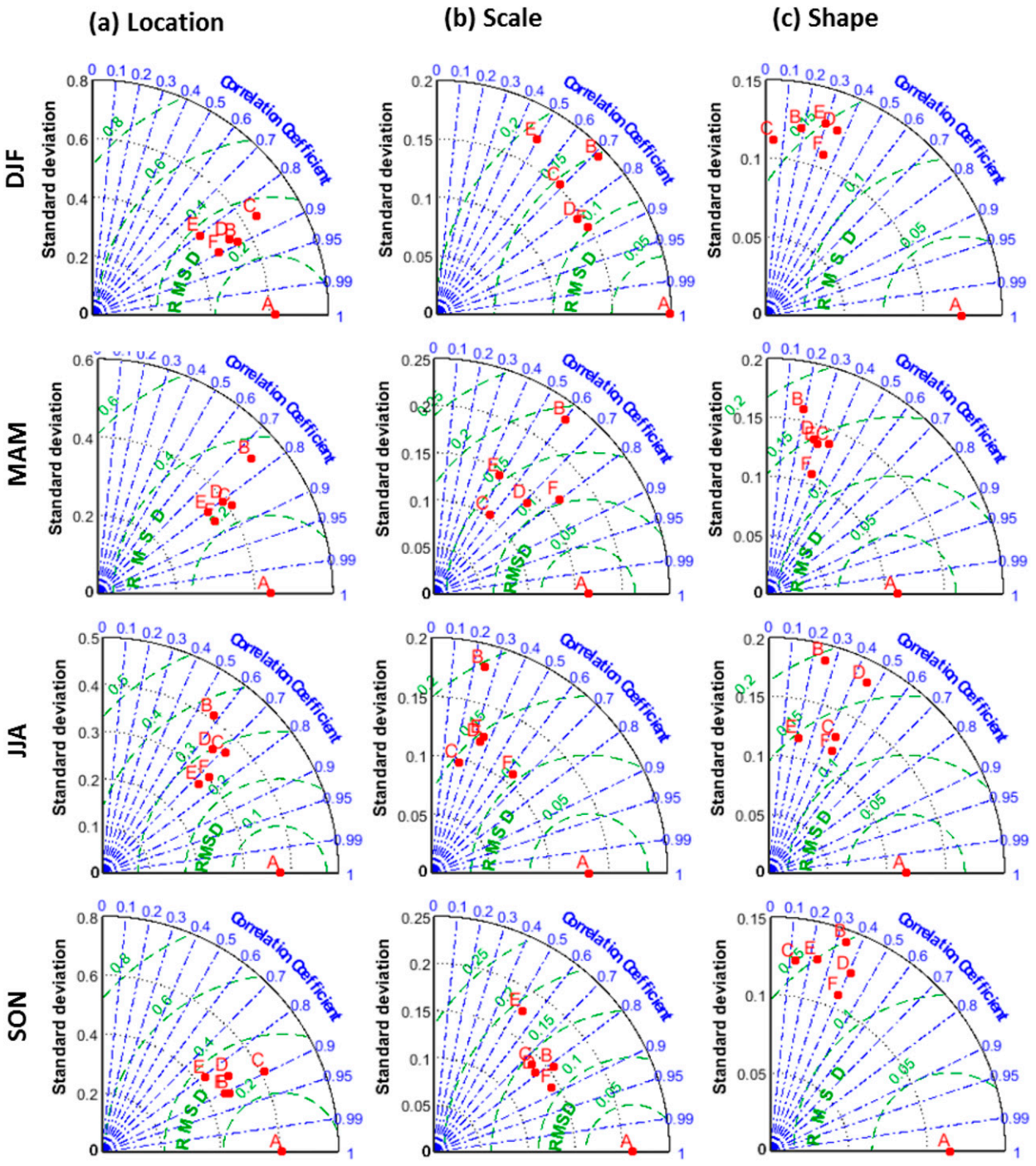

FIG. 5. Taylor diagrams showing the spatial standard deviation (black arcs), the spatial root-mean-square differences (green arcs), and the spatial correlation (blue arcs) of the three GEV parameter estimates of PE relative to the MSWEP-ERA (point A) parameter estimates for CanRCM4 (point B), CRCM5 (point C), ERA-Interim (point D), NARR (point E), and CFSR (point F) for each season: winter (DJF), spring (MAM), summer (JJA), and autumn (SON).

for CRCM5 are seen in the Desert region during the spring and fall seasons, the PacificSW region during the winter and the MtWest region during the summer. For CanRCM4, the largest biases in PE shape parameter estimates compared to the other models are in the opposite direction, with overestimations in the Desert region during the spring and in the MtWest region during the summer.

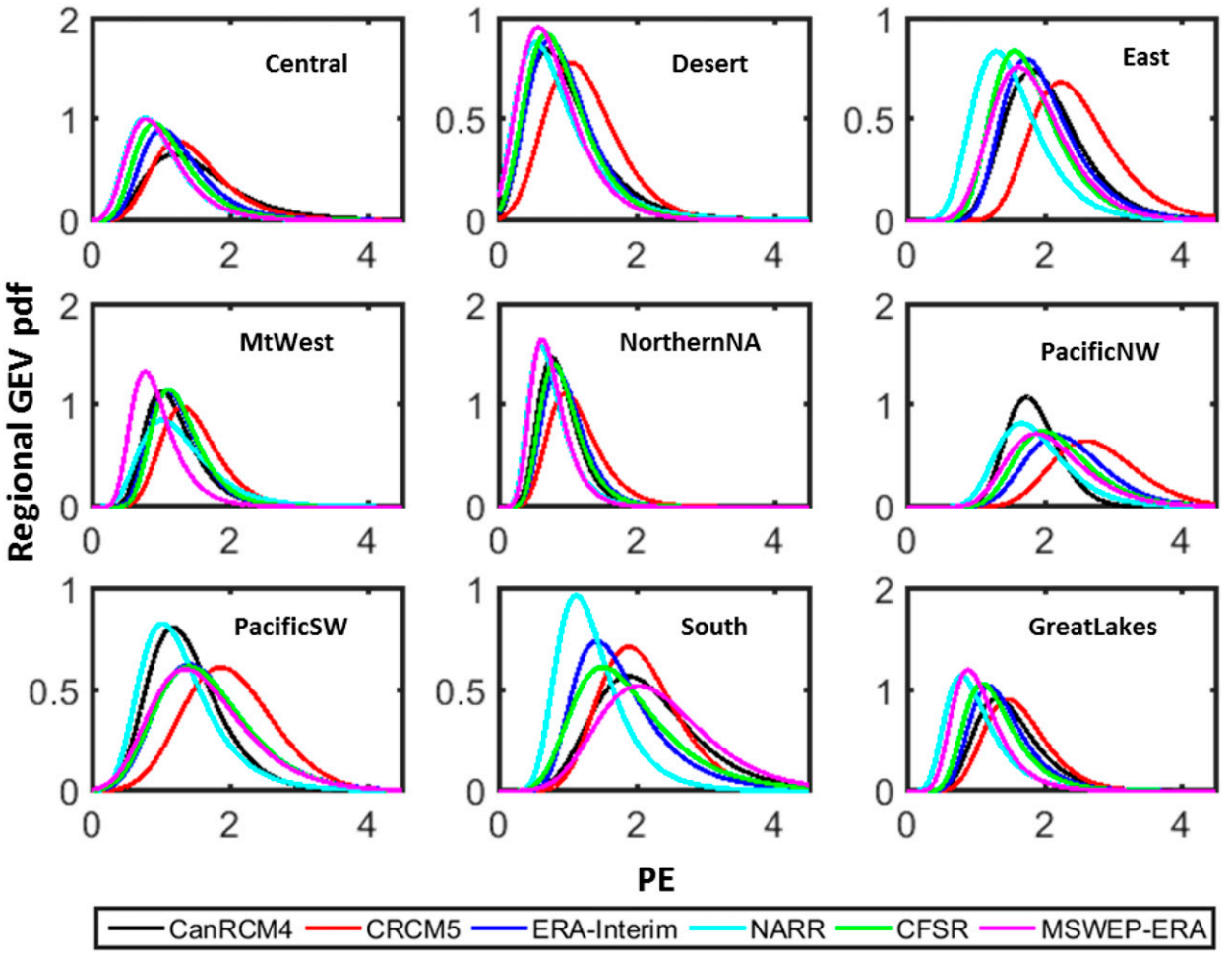

FIG. 6. PDF plots of the regional precipitation efficiency GEV distribution for both RCMs, reanalyses, and MSWEP-ERA during DJF.

c. *Extreme dependence results*

We next consider the Gumbel copulas for each grid box using the procedure described in section 2. The joint occurrence of extreme events can be measured by the so-called upper tail dependence (UTD) coefficient λ_U. For a bivariate extremes copula, this coefficient can be obtained from the Pickands dependence function as (Salvadori et al. 2007):

$$\lambda_U = 2 - 2A(1/2). \tag{4}$$

The UTD coefficient varies between 0 (in the case of independence) and 1 (in the case of total dependence). Maps that display the coefficient values obtained from the fitted Gumbel copulas are presented in Fig. 8 for each season. Although the UTD coefficient does not exhibit a strong spatial pattern, the two RCMs seem to be in a good agreement with the three reanalyses and MSWEP-ERA. Generally UTD values are very low, suggesting that the total dependence assumption for PE and PW extremes is likely not valid. The mean UTD values over North America vary between 0.08 in CRCM5 during the winter and 0.15 in ERA-Interim during the summer.

d. *Probable maximum precipitation results*

It is desirable to quantify how these results could affect PMP estimates from CanRCM4 and CRCM5. Since the RCMs and reanalyses all exhibit similar precipitable water extreme values, the dissimilarity between them will be mainly related to their ability to simulate extreme precipitation efficiency. Hence, 1000 values were sampled from the estimated PMP distribution for each grid box for each of the RCMs and reanalysis products using the algorithm proposed in section 2. The main advantage of the probabilistic approach is that it allows evaluation of the uncertainty inherent in PMP estimates. Indeed, these samples once obtained, can then be used to estimate the properties of the PMP distribution (e.g., mean, mode, median, and quantiles). Figure 9 shows maps of the range

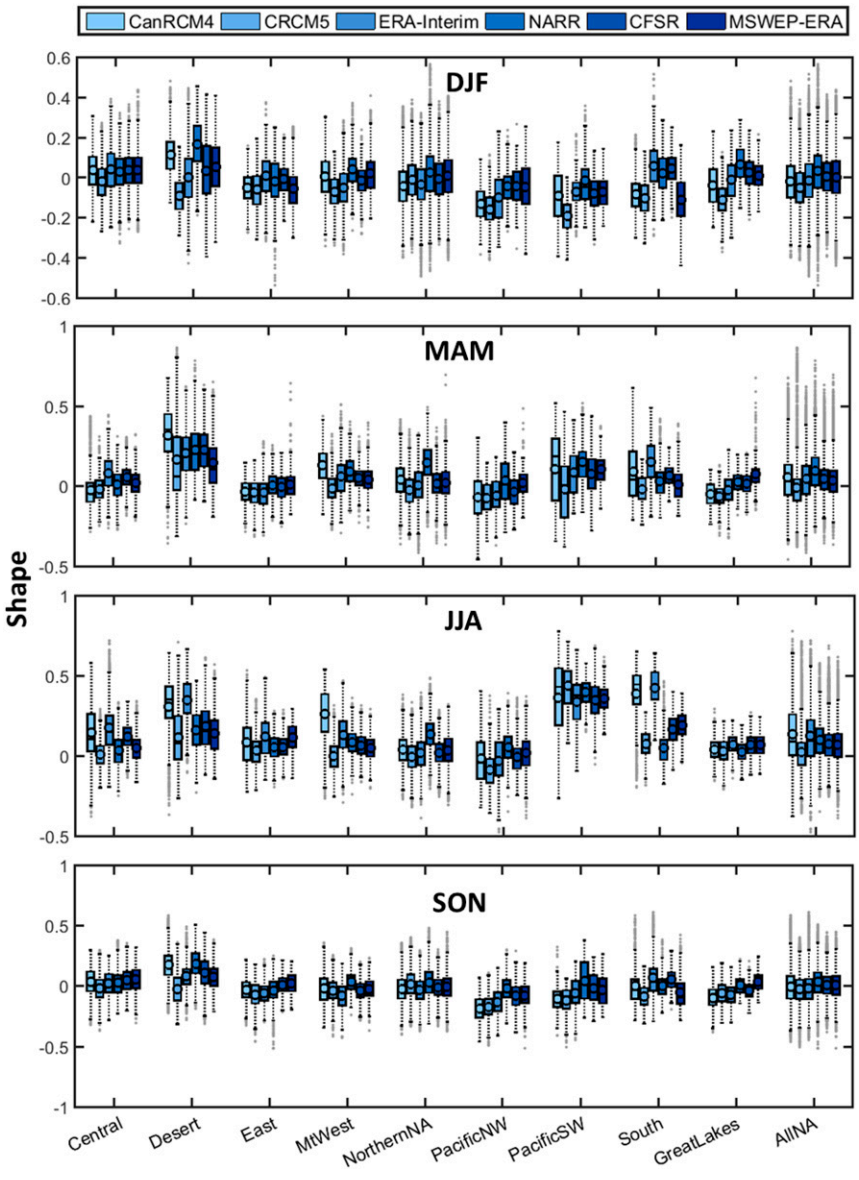

FIG. 7. Boxplots of estimated shape parameter for PE for each season and each Bukovsky region for both RCMs, reanalyses, and MSWEP-ERA.

of plausible PMP values corresponding to the 10th, 50th, and 90th percentiles. Similar maps for 24-h PMP estimates are also shown in the supplemental material (see Fig. S14). As expected, PMP estimates based on $m = 100$ years have large uncertainties as indicated by the 80% confidence intervals that are bounded by the 10th and 90th percentiles. The spatial patterns seen in the maps of the three PMP percentiles are reasonably consistent across RCMs and reanalysis products on the continental scale and the largest PMP values are found on the southeast of the continent. As we can see from Fig. 9, the differences in PMP magnitudes between the reanalysis products seems to be as large as those between RCMs. MSWEP-ERA seems to be close to the reanalysis consensus, thus suggesting that we may have a bit more confidence in this hybrid dataset than the reanalyses. The high correlation coefficients shown in the Taylor diagrams (Taylor 2001) for the 10th, 50th, and 90th PMP percentiles confirm the finding that spatial patterns are very similar (see Fig. 10).

For comparison purposes, Fig. 9 (as well Fig. S14 for 24-h PMP estimates) also shows PMP estimates for 12 selected basins in the United States that were obtained from the NOAA Hydrometeorological Reports (HMRs) and are based on the moisture maximization approach (Schreiner and Riedel 1978). Table 2 shows 6-h and daily

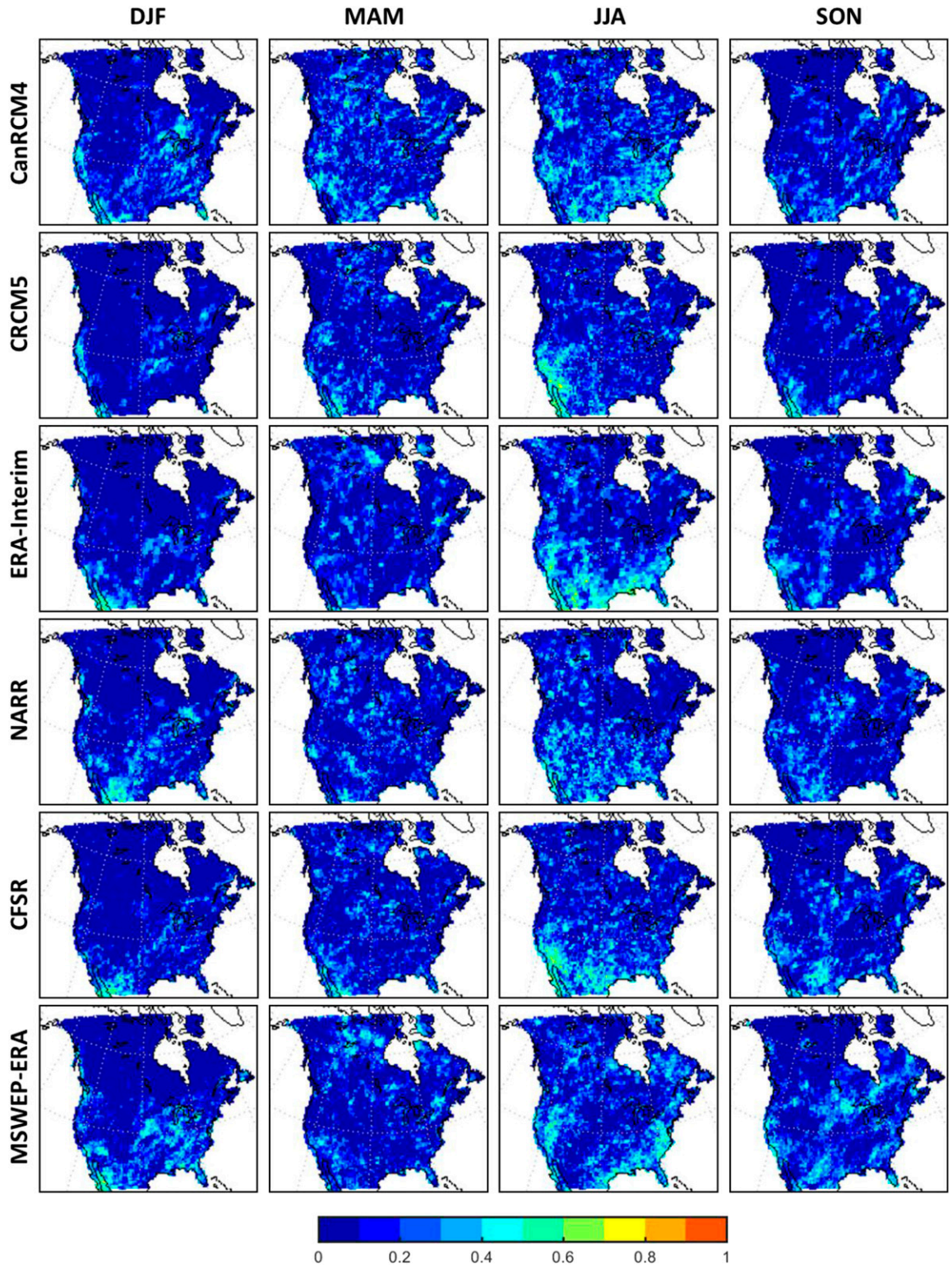

FIG. 8. Estimated UTD coefficient for PE for both RCMs, reanalyses, and MSWEP-ERA for each season.

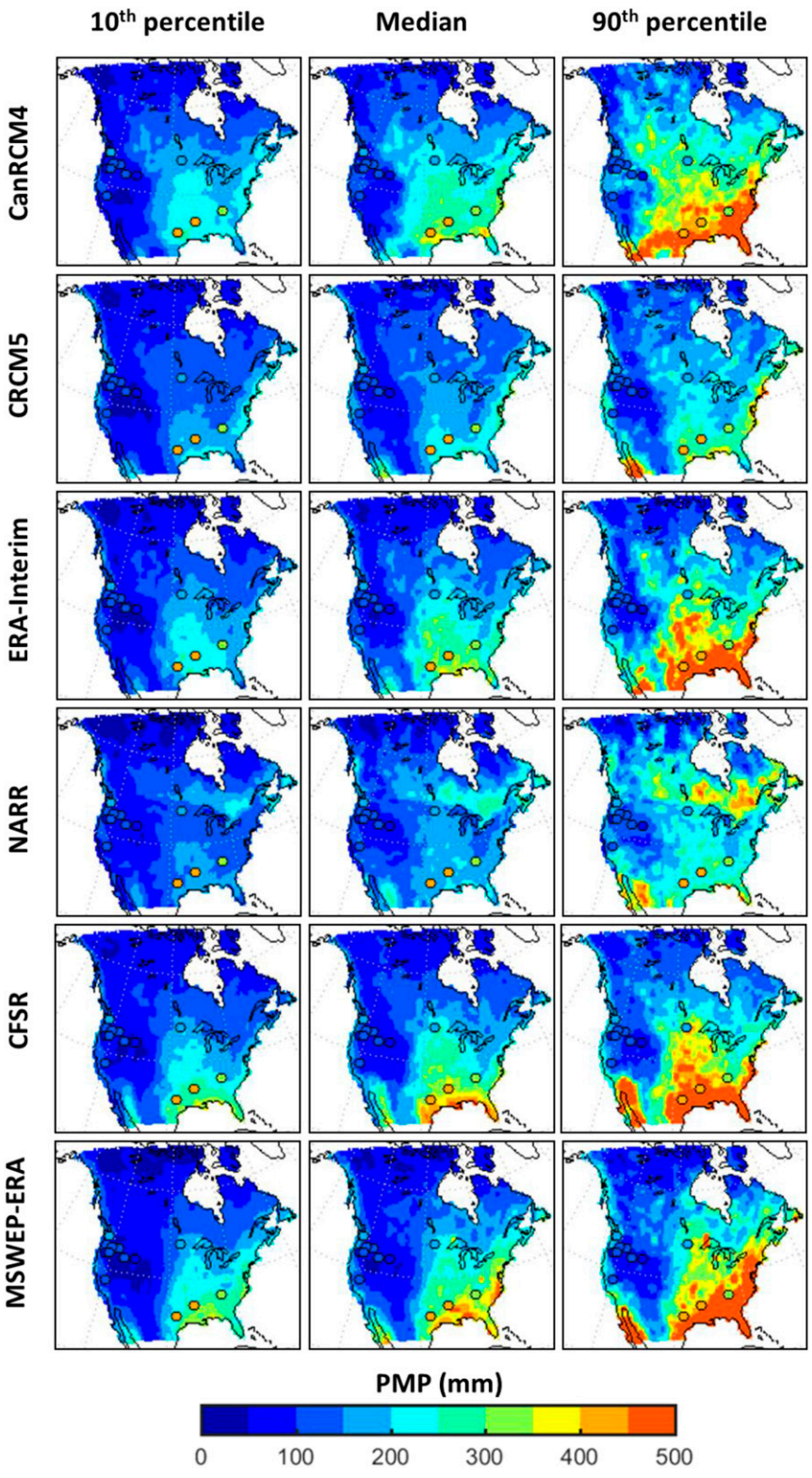

FIG. 9. Estimated 6-h PMP percentiles using the bivariate GEV model for both RCMs, reanalyses, and MSWEP-ERA over North America. Circles denote HMR estimates presented in Table 3.

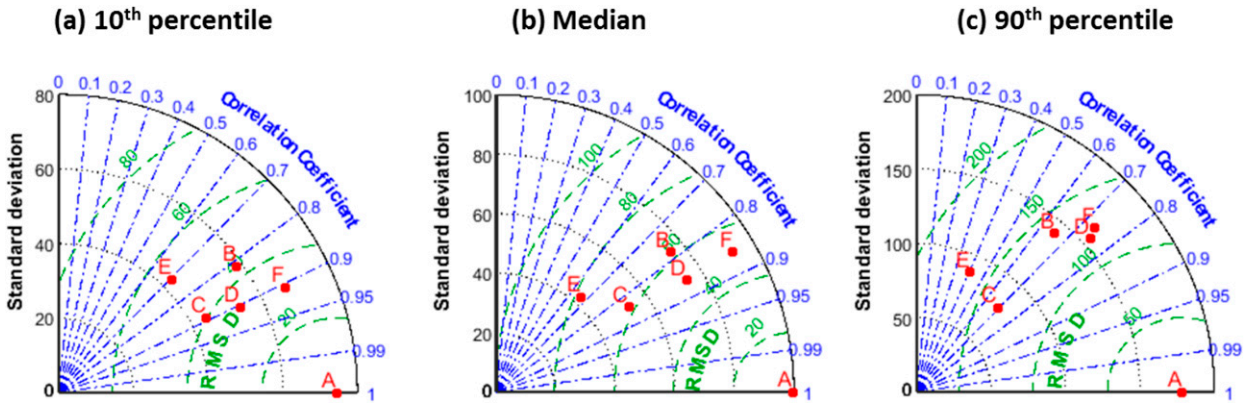

FIG. 10. Taylor diagrams showing the spatial standard deviation (black arcs), the spatial root-mean-square differences (green arcs), and the spatial correlation (blue arcs) of PMP percentiles relative to the corresponding MSWEP-ERA (point A) PMP percentiles for CanRCM4 (point B), CRCM5 (point C), ERA-Interim (point D), NARR (point E), and CFSR (point F).

PMP values for each basin together with some basin characteristics, including geographical location, area, the reference number of the HMR document from which the PMP values were abstracted, and the Bukovsky region that corresponds to each basin. Our selection of basins was mainly based on area so that it is somewhat comparable with the spatial resolution of the RCMs. Note that climate-model-based PMP estimates and HMR estimates are calculated differently. Indeed, HMR estimates are obtained from historical observations for a different period, use dewpoint temperature and assume pseudoadiabatic conditions. In addition, HMR estimates involve professional judgements and several steps that are specific to the target basin. Nevertheless, evaluating the consistency of climate-model-based PMP estimates with traditional values that have been used in the infrastructure design is somewhat helpful in understanding climate-model-based PMP estimates and whether they can be used operationally by practitioners. To our best knowledge, only a few studies have dealt with this issue (e.g., Chen et al. 2017; Rastogi et al. 2017). As we can see from Fig. 9 (and Fig. S14), despite the high variation in HMR 6-h (and 24-h) PMP estimates, all six models acceptably reproduce the spatial pattern and the high heterogeneity of the PMP magnitudes. In general, single-value HMR PMP estimates lie well within the range of the PMP distribution obtained from the climate models. Nevertheless, for both 6- and 24-h PMP estimates, a strong negative bias were identified for both regional and reanalysis models in the South and East region. In particular, HMR estimates are shown to exceed the 90th PMP estimated for NARR, ERA-Interim, and CRCM5 in the South and East regions. One reasonable explanation of this bias is the relatively coarse spatial resolution of the used climate models. Indeed, given their 50-km spatial resolution, the regional climate models used in our analysis are not expected to skillfully simulate all phenomena that, in nature, are responsible for extreme precipitation at finer scales. One reason is that precipitation is influenced by vertical motions and microphysical process occurring at scales smaller than the model grid (Wehner et al. 2010). Furthermore, precipitation is often influenced by orography, which is smoothed by the finite grid sizes used in climate models.

TABLE 2. HMR estimates for the 12 selected basins.

Basin	Latitude (°N)	Longitude (°W)	Bukovsky region	Area (km^2)	HMR document	6-h PMP (mm)	24-h PMP (mm)
Anderson Ranch	43.35	115.44	MtWest	2548	57	124.96	264.41
Thief Valley	45.01	117.78	MtWest	2366	57	105.15	231.39
Ririe	43.58	111.74	MtWest	2072	57	85.09	192.53
Leon River	31.1	97.47	South	2600	52	411.48	538.48
Knoxville Airport	35.81	83.99	East	2600	56	340.36	520.70
Auburne drainage	47.33	122.28	MtWest	2529	59	175.26	434.84
Clear Lake	48.55	122.22	PacificNW	1911	59	83.05	171.95
New Melones	38.15	120.52	MtWest	2350	59	139.7	360.93
Tuitchell	34.99	120.33	PacificSW	2951	59	119.3	278.63
Ouachita River	33.92	92.46	South	2600	52	414.02	642.62
Red Lake River	47.77	96.61	Central	2080	48	195.58	294.64
Friant	37.18	119.69	MtWest	4134	59	134.11	355.09

Very finescale models such as Weather Research and Forecasting (WRF) simulations at convection permitting scales may allow PMP estimation across a wider range of scales, perhaps even allowing exploratory ''site-specific'' PMP estimates. For instance, Rastogi et al. (2017) conducted WRF simulations to derive site-specific PMP estimates at 3-km horizontal resolution that were subsequently used by Gangrade et al. (2018) for PMF studies using the Distributed Hydrology Soil Vegetation Model (DHSVM) at a fine 90-m horizontal resolution.

Despite, their lower resolution, regional climate models using conventional parameterizations of convection remain very useful for studying ''generalized PMP estimates'' (e.g., Schreiner and Riedel 1978) over larger regions. As described in Schreiner and Riedel (1978), at site HMR PMP estimates that have been used in the infrastructure design stage are obtained after estimating generalized PMP estimates at larger scales and then removing generalization on a case by case basis. The mapping from generalized PMP estimates to site-specific estimates is conducted through one or more adjustment factors that are functions of the formative components of the physical processes involved at the specific designated region together with their spatial extents and more detailed information about the orography. Those adjustment factors are already available for HMR sites and are derived from observations not from climate models. Therefore, future generalized PMP estimates can be obtained from future climate simulations, while future site-specific PMP estimates can be derived by removing the generalization, in a downscaling perspective, using the already available adjustment factors. In addition regional climate models are also useful for providing generalized guidance on a continental scale. Our choice to use a 3×3 grid box (approximately 150 km $\times$ 150 km) moving window and the parameter $m = 100$ within our simplified moisture maximization approach is motivated by the desire to provide general guidelines over North America.

Table 3 shows the relative bias (RBIAS) in percent of the mean value of simulated PMP values, using MSWEP-ERA as a reference. CRCM5 has a tendency to underestimate the mean PMP value, except in the MtWest and NorthernNA regions. This negative bias is particularly important in the South (−41%), GreatLakes (−29%), and East (−27%) regions. On the other hand the three largest biases of CanRCM4 are the overestimation by 74% in MtWest and 41% in Central, and the underestimation by 30% respectively in the PacificNW and PacificSW regions. On the continental scale over North America, CRCM5 has a tendency to modestly underestimate PMP by ~5% while CanRCM4 has a tendency for overestimation by ~22%. Generally CRCM5 shows good agreement with ERA-Interim, while CanRCM4 is more comparable to CFSR.

TABLE 3. Relative bias (RBIAS) of CanRCM4/CRCM5 compared reanalysis products in simulating the PMP mean value for each region and over all North America (AllNA) in percent (%).

	Model				
Region	CanRCM4	CRCM5	ERA-Interim	NARR	CFSR
Central	41	−5	20	−2	23
Desert	4	−20	0	3	33
East	−9	−27	−25	−38	−27
MtWest	74	8	23	40	19
NorthernNA	28	17	9	20	10
PacificNW	−30	−10	−12	−3	−11
PacificSW	−30	−3	−6	25	−2
South	−20	−41	−18	−45	0
GreatLakes	−5	−29	−14	−27	−12
AllNA	22	−5	−2	4	9

Finally, GEV parameters were averaged on a regional basis. Based on the averaged parameters, 1000 random regional PMP values were simulated from these regionally averaged bivariate GEV parameters to estimate the regional PMP probability density function (PDF). As shown in Fig. 11, the regional PMP distributions are positively skewed for all models. CRCM5 corresponds well with ERA-Interim in reproducing the PDF form of the regional PMP, in most regions, except for the Central, South, and GreatLakes regions. CanRCM4, however, is more comparable to CFSR. In most regions, except in the two Pacific regions (PacificNW and PacificSW), the CanRCM4 and CFSR PDFs are wider and have heavier upper tails than the CRCM5, ERA-Interim, and NARR PDFs. This implies additional uncertainty where high PMP values are more likely, as shown in Fig. 9 where the 80% confidence intervals are presented.

We recognize the PMP concept emerged long before multivariate extreme value theories were developed. The approaches that are used by practitioners, which are often embedded in standards, have treated PMP estimation as a deterministic problem, as is recognized, for example, by Rastogi et al. (2017). Casting the problem in a stochastic framework allows us to take advantage of recent development in multivariate extreme value analysis and provides a means for dealing the estimation and interpretation of PMP in a warming climate. Nevertheless, the literature suggests that it is best to stay as close as possible to the traditional method used by standards setting organizations when using a

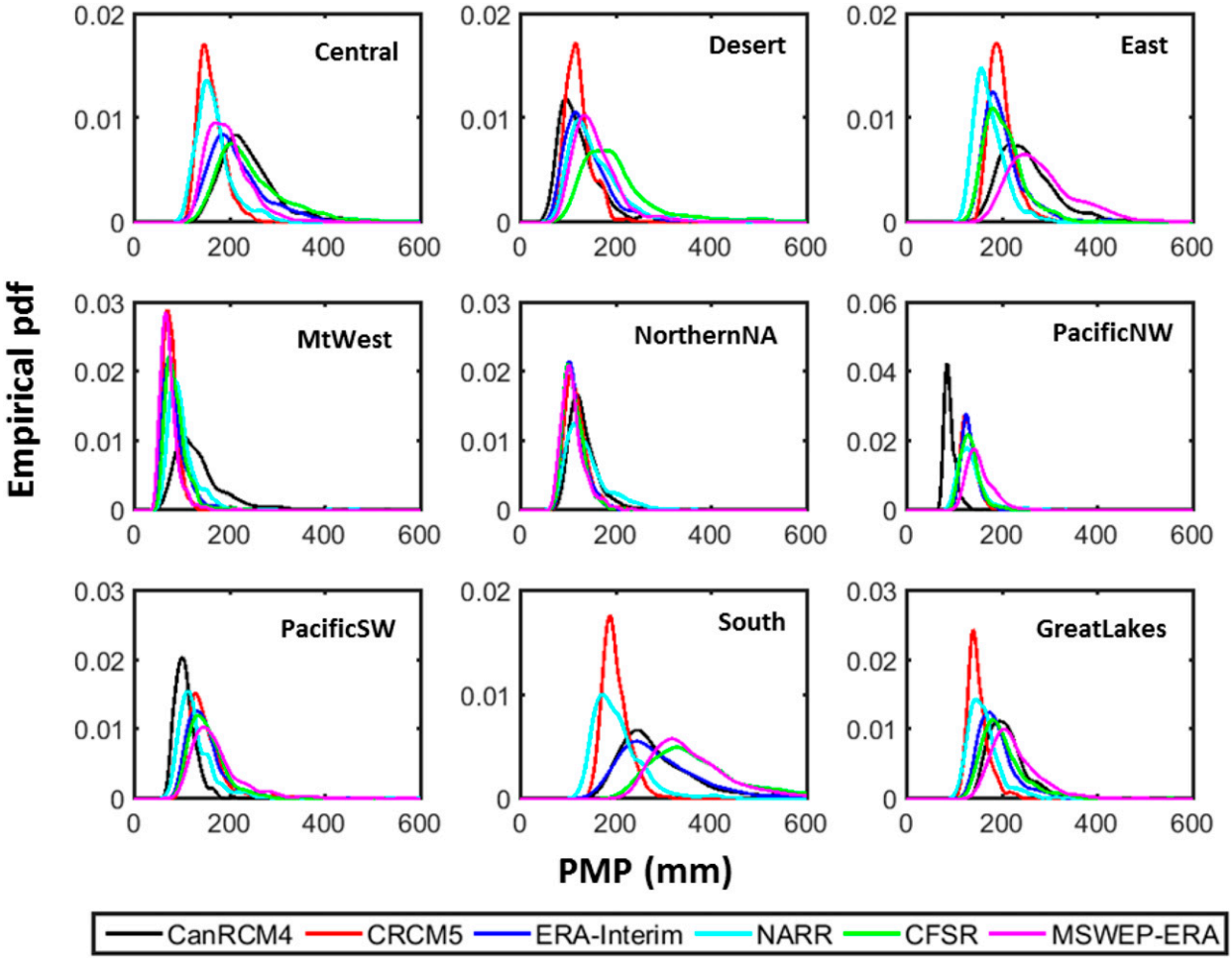

FIG. 11. PDF plots of the regional PMP distribution for both RCMs, reanalyses, and MSWEP-ERA.

climate model to derive PMP estimates (Clavet-Gaumont et al. 2017). Maintaining greater consistency with the traditional practice will require us to restrict the multivariate probabilistic analysis to high efficiency values that also have high absolute values of rainfall accumulation. Accounting for seasonality as we have done is a step in this direction. We will be pursuing this further in a subsequent paper, as discussed previously (Ben Alaya et al. 2018).

While this paper has focused on all-season PMP estimates (meaning the highest value over all seasons), we recognize that it may be necessary to determine the seasonal variations of PMP. For example, in regions where contributions to large river flows may be the result of simultaneous occurrences of snowmelt and rainfall, a key concern would be to obtain PMP estimates that are appropriate to the melting season. While this is not shown in the current analysis, Fig. S15 demonstrates the high consistency between all six models used in our analysis in simulating the occurrence probability of all season PMP events for each season.

4. Conclusions

Updating PMP estimates to consider future climate conditions is a growing concern due to the need to assess infrastructures safety in the context of a warming climate. RCM simulations represent a potentially useful way to derive PMP estimates corresponding to future climate conditions. However, before RCMs can be used for this purpose, their ability to provide PMP estimates for the present climate must be assessed. Even if the current knowledge of storm mechanisms remains insufficient to properly evaluate the limiting values of extreme precipitation, PMP estimation methods still view the problem from a deterministic perspective, and thus give only single values without uncertainty estimates. In this study we have compared PMP estimates over North America based on historical climate

simulations with two Canadian regional climate models (CanRCM4 and CRCM5) and three reanalyses: ERA-Interim, NARR, and CFSR. A hybrid dataset combining precipitation from MSWEP and PW from ERA-Interim was also considered. PMP estimates from all datasets were developed using a probabilistic extension of the usual moisture maximization method that was recently proposed by Ben Alaya et al. (2018). The latter uses the Gumbel copula to combine two GEV models that are separately fitted to the seasonal maxima of PE and PW and thus attempts to take advantage of bivariate extreme value analysis to explore uncertainty and to provide ranges of PMP values that reflect the resampling uncertainty due to the data used in PMP estimation.

In a first step of the assessment, the two RCMs were compared to the three sets of reanalysis based on their ability to reproduce the three components of the bivariate GEV distribution. Main results show that the two RCMs are able to reproduce the spatial pattern of each component reasonably well. The PW extremes and the dependence structure of extreme PW and PE are well simulated by both RCMs. The strength of the dependence, which is measured by the upper tail dependence function between the extremes of PE and PW is low and demonstrates that the assumption of the total dependence between PE and PW extremes that is made in the usual operational PMP estimation approach may not be valid. The biases that are present in PMP estimated by both RCMs are mainly related to their abilities to simulate extreme precipitation efficiency. A main result is that the spatial pattern of the PMP derived from the two RCMs is in a good agreement with reanalyses products and MSWEP-ERA. On the other hand, both RCMs have PMP magnitude biases, with regional and model differences in the sign of the bias. The largest biases are the underestimation by CRCM5 in the South and Great Lakes regions and by CanRCM4 in the Pacific Northwest and Pacific Southwest regions, and the overestimation by CanRCM4 in the Mountain West region.

While the comparison with reanalysis products and MSWEP-ERA is far from perfect given that precipitation is only weakly constrained by observations in reanalyses, the main results suggest that the RCMs perform well enough to allow users to have some confidence in projected changes in generalized PMP estimates that can be obtained via our probabilistic approach. Further, the approach that we have demonstrated allows the assessment of differences between models, or when considering the future, between projections, that accounts for the large sampling uncertainty that is inherent in PMP estimates. In contrast to traditional, operational approaches, the method that is described in Ben Alaya et al. (2018) and is applied here, allows quantification of the large uncertainties associated with sampling errors, which is a necessary prerequisite for the interpretation of differences between projections from different models and under different emissions scenarios.

Acknowledgments. We thank Alex Cannon and Vincent Cheng from Environment and Climate Change Canada for their comments that helped to improve this paper. We thank three anonymous reviewers for their careful reading of our manuscript and their many insightful comments and suggestions.

REFERENCES

Beauchamp, J., R. Leconte, M. Trudel, and F. Brissette, 2013: Estimation of the summer-fall PMP and PMF of a northern watershed under a changed climate. *Water Resour. Res.*, **49**, 3852–3862, https://doi.org/10.1002/wrcr.20336.

Beck, H. E., A. I. van Dijk, V. Levizzani, J. Schellekens, D. G. Miralles, B. Martens, and A. de Roo, 2017: MSWEP: 3-hourly 0.25 global gridded precipitation (1979–2015) by merging gauge, satellite, and reanalysis data. *Hydrol. Earth Syst. Sci.*, **21**, 589–615, https://doi.org/10.5194/hess-21-589-2017.

Beirlant, J., Y. Goegebeur, J. Segers, and J. Teugels, 2006: *Statistics of Extremes: Theory and Applications*. John Wiley & Sons, 514 pp.

Ben Alaya, M. A., F. W. Zwiers, and X. Zhang, 2018: Probable maximum precipitation: Its estimation and uncertainty quantification using bivariate extreme value analysis. *J. Hydrometeor.*, **19**, 679–694, https://doi.org/10.1175/JHM-D-17-0110.1.

Benson, A. M., 1973: Thoughts on the design of design floods. *Floods and Droughts, Proceedings of the 2nd International Symposium in Hydrology*, Water Resources Publications, 27–33.

Bukovsky, M., 2012: Masks for the Bukovsky regionalization of North America, Regional Integrated Sciences Collective. Institute for Mathematics Applied to Geosciences, National Center for Atmospheric Research, accessed 3 July 2019, http://www.narccap.ucar.edu/contrib/bukovsky/.

Capéraà, P., A.-L. Fougères, and C. Genest, 1997: A nonparametric estimation procedure for bivariate extreme value copulas. *Biometrika*, **84**, 567–577, https://doi.org/10.1093/biomet/84.3.567.

Chen, X., and F. Hossain, 2018: Understanding model-based probable maximum precipitation estimation as a function of location and season from atmospheric reanalysis. *J. Hydrometeor.*, **19**, 459–475, https://doi.org/10.1175/JHM-D-17-0170.1.

——, ——, and L. R. Leung, 2017: Probable maximum precipitation in the US Pacific Northwest in a changing climate. *Water Resour. Res.*, **53**, 9600–9622, https://doi.org/10.1002/2017WR021094.

Clavet-Gaumont, J., and Coauthors, 2017: Probable maximum flood in a changing climate: An overview for Canadian basins. *J. Hydrol. Reg. Stud.*, **13**, 11–25, https://doi.org/10.1016/j.ejrh.2017.07.003.

Coles, S., J. Bawa, L. Trenner, and P. Dorazio, 2001: *An Introduction to Statistical Modeling of Extreme Values*. Springer, 209 pp.

Collins, M., and Coauthors, 2013: Long-term climate change: Projections, commitments and irreversibility. *Climate Change 2013: The Physical Science Basis*, T. F. Stocker et al., Eds., Cambridge University Press, 1029–1136.

Côté, J., S. Gravel, A. Méthot, A. Patoine, M. Roch, and A. Staniforth, 1998: The operational CMC-MRB global environmental multiscale (GEM) model. Part I: Design considerations and formulation. *Mon. Wea. Rev.*, **126**, 1373–1395, https://doi.org/10.1175/1520-0493(1998)126<1373:TOCMGE>2.0.CO;2.

Dee, D., and Coauthors, 2011: The ERA-Interim reanalysis: Configuration and performance of the data assimilation system. *Quart. J. Roy. Meteor. Soc.*, **137**, 553–597, https://doi.org/10.1002/qj.828.

Dingman, S. L., 2008: *Physical Hydrology*. 2nd ed. Waveland Press, 656 pp.

Dupuis, D., and M. Tsao, 1998: A hybrid estimator for generalized Pareto and extreme-value distributions. *Commun. Stat. Theory Methods*, **27**, 925–941, https://doi.org/10.1080/03610929808832136.

Embrechts, P., C. Klüppelberg, and T. Mikosch, 2013: *Modelling Extremal Events: For Insurance and Finance*. Springer, 648 pp.

Foufoula-Georgiou, E., 1989: A probabilistic storm transposition approach for estimating exceedance probabilities of extreme precipitation depths. *Water Resour. Res.*, **25**, 799–815, https://doi.org/10.1029/WR025i005p00799.

Gangrade, S., S. C. Kao, B. S. Naz, D. Rastogi, M. Ashfaq, N. Singh, and B. L. Preston, 2018: Sensitivity of probable maximum flood in a changing environment. *Water Resour. Res.*, **54**, 3913–3936, https://doi.org/10.1029/2017WR021987.

Genest, C., and L.-P. Rivest, 1993: Statistical inference procedures for bivariate Archimedean copulas. *J. Amer. Stat. Assoc.*, **88**, 1034–1043, https://doi.org/10.1080/01621459.1993.10476372.

——, and J. Segers, 2009: Rank-based inference for bivariate extreme-value copulas. *Ann. Stat.*, **37**, 2990–3022, https://doi.org/10.1214/08-aos672.

Giorgi, F., C. Jones, and G. R. Asrar, 2009: Addressing climate information needs at the regional level: The CORDEX framework. *WMO Bull.*, **58** (3), 175.

Hernández-Díaz, L., R. Laprise, L. Sushama, A. Martynov, K. Winger, and B. Dugas, 2013: Climate simulation over CORDEX Africa domain using the fifth-generation Canadian Regional Climate Model (CRCM5). *Climate Dyn.*, **40**, 1415–1433, https://doi.org/10.1007/s00382-012-1387-z.

Hosking, J. R. M., 1990: L-moments: Analysis and estimation of distributions using linear combinations of order statistics. *J. Roy. Stat. Soc.*, **52B**, 105–124.

Kalnay, E., and Coauthors, 1996: The NCEP/NCAR 40-Year Reanalysis Project. *Bull. Amer. Meteor. Soc.*, **77**, 437–471, https://doi.org/10.1175/1520-0477(1996)077<0437:TNYRP>2.0.CO;2.

Kite, G. W., 1988: *Frequency and Risk Analyses in Hydrology*. Water Resources Publications, 257 pp.

Koutsoyiannis, D., 1999: A probabilistic view of Hershfield's method for estimating probable maximum precipitation. *Water Resour. Res.*, **35**, 1313–1322, https://doi.org/10.1029/1999WR900002.

Kunkel, K. E., T. R. Karl, D. R. Easterling, K. Redmond, J. Young, X. Yin, and P. Hennon, 2013: Probable maximum precipitation and climate change. *Geophys. Res. Lett.*, **40**, 1402–1408, https://doi.org/10.1002/grl.50334.

Laprise, R., L. Hernández-Díaz, K. Tete, L. Sushama, L. Šeparović, A. Martynov, K. Winger, and M. Valin, 2013: Climate projections over CORDEX Africa domain using the fifth-generation Canadian Regional Climate Model (CRCM5). *Climate Dyn.*, **41**, 3219–3246, https://doi.org/10.1007/s00382-012-1651-2.

Mesinger, F., G. DiMego, E. Kalnay, and K. Mitchell, 2006: North American regional reanalysis. *Bull. Amer. Meteor. Soc.*, **87**, 343–360, https://doi.org/10.1175/BAMS-87-3-343.

Micovic, Z., M. G. Schaefer, and G. H. Taylor, 2015: Uncertainty analysis for probable maximum precipitation estimates. *J. Hydrol.*, **521**, 360–373, https://doi.org/10.1016/j.jhydrol.2014.12.033.

Mo, K. C., M. Chelliah, M. L. Carrera, R. W. Higgins, and W. Ebisuzaki, 2005: Atmospheric moisture transport over the United States and Mexico as evaluated in the NCEP regional reanalysis. *J. Hydrometeor.*, **6**, 710–728, https://doi.org/10.1175/JHM452.1.

Ohara, N., M. Kavvas, S. Kure, Z. Chen, S. Jang, and E. Tan, 2011: Physically based estimation of maximum precipitation over American River watershed, California. *J. Hydrol. Eng.*, **16**, 351–361, https://doi.org/10.1061/(ASCE)HE.1943-5584.0000324.

Papalexiou, S., and D. Koutsoyiannis, 2006: A probabilistic approach to the concept of Probable Maximum Precipitation. *Adv. Geosci.*, **7**, 51–54, https://doi.org/10.5194/adgeo-7-51-2006.

Paquin, D., A. Frigon, and K. Kunkel, 2016: Evaluation of total precipitable water from CRCM4 using the NVAP-MEaSUREs Dataset and ERA-Interim reanalysis data. *Atmos.–Ocean*, **54**, 541–548, https://doi.org/10.1080/07055900.2016.1230043.

Rakhecha, P., and C. Clark, 1999: Revised estimates of one-day probable maximum precipitation (PMP) for India. *Meteor. Appl.*, **6**, 343–350, https://doi.org/10.1017/S1350482799001280.

Rastogi, D., and Coauthors, 2017: Effects of climate change on probable maximum precipitation: A sensitivity study over the Alabama-Coosa-Tallapoosa River Basin. *J. Geophys. Res. Atmos.*, **122**, 4808–4828, https://doi.org/10.1002/2016JD026001.

Rouhani, H., and R. Leconte, 2016: A novel method to estimate the maximization ratio of the Probable Maximum Precipitation (PMP) using regional climate model output. *Water Resour. Res.*, **52**, 7347–7365, https://doi.org/10.1002/2016WR018603.

Rousseau, A. N., I. M. Klein, D. Freudiger, P. Gagnon, A. Frigon, and C. Ratté-Fortin, 2014: Development of a methodology to evaluate probable maximum precipitation (PMP) under changing climate conditions: Application to southern Quebec, Canada. *J. Hydrol.*, **519**, 3094–3109, https://doi.org/10.1016/j.jhydrol.2014.10.053.

Saha, S., and Coauthors, 2010: The NCEP Climate Forecast System Reanalysis. *Bull. Amer. Meteor. Soc.*, **91**, 1015–1058, https://doi.org/10.1175/2010BAMS3001.1.

Salas, J. D., and F. R. Salas, 2016: Estimating the uncertainty of the PMP. *XXVII IAHR Latin American Congress of Hydraulics*, Lima, Peru, IAHR.

——, G. Gavilán, F. R. Salas, P. Y. Julien and J. Abdullah, 2014: Uncertainty of the PMP and PMF. *Handbook of Engineering Hydrology*, S. Eslamian, Ed., CRC Press, 575–603.

Salvadori, G., C. De Michele, N. T. Kottegoda, and R. Rosso, 2007: *Extremes in Nature: An Approach Using Copulas*. Springer, 292 pp.

Schreiner, L. C., and J. T. Riedel, 1978: Probable maximum precipitation estimates, United States east of the 105th meridian. NOAA Hydrometeorological Rep. 51, 87 pp., https://www.nws.noaa.gov/oh/hdsc/PMP_documents/HMR51.pdf .

Scinocca, J., and Coauthors, 2016: Coordinated global and regional climate modeling. *J. Climate*, **29**, 17–35, https://doi.org/10.1175/JCLI-D-15-0161.1.

Šeparović, L., A. Alexandru, R. Laprise, A. Martynov, L. Sushama, K. Winger, K. Tete, and M. Valin, 2013: Present climate and climate change over North America as simulated by the fifth-generation Canadian regional climate model. *Climate Dyn.*, **41**, 3167–3201, https://doi.org/10.1007/s00382-013-1737-5.

Serinaldi, F., 2008: Analysis of inter-gauge dependence by Kendall's τ_K, upper tail dependence coefficient, and 2-copulas with application to rainfall fields. *Stochastic Environ. Res. Risk Assess.*, **22**, 671–688, https://doi.org/10.1007/s00477-007-0176-4.

Shaw, E. M., K. J. Beven, N. A. Chappell, and R. Lamb, 2010: *Hydrology in Practice*. 4th ed. CRC Press, 560 pp.

Taylor, K. E., 2001: Summarizing multiple aspects of model performance in a single diagram. *J. Geophys. Res.*, **106**, 7183–7192, https://doi.org/10.1029/2000JD900719.

Wehner, M. F., R. L. Smith, G. Bala, and P. Duffy, 2010: The effect of horizontal resolution on simulation of very extreme US precipitation events in a global atmosphere model. *Climate Dyn.*, **34**, 241–247, https://doi.org/10.1007/s00382-009-0656-y.

Whan, K., and F. Zwiers, 2016: Evaluation of extreme rainfall and temperature over North America in CanRCM4 and CRCM5. *Climate Dyn.*, **46**, 3821–3843, https://doi.org/10.1007/s00382-015-2807-7.

WMO, 2009: Manual on estimation of probable maximum precipitation (PMP). Tech. Rep. WMO-1045, 257 pp., http://www.wmo.int/pages/prog/hwrp/publications/PMP/WMO%201045%20en.pdf.

Yang, L., and J. Smith, 2018: Sensitivity of extreme rainfall to atmospheric moisture content in the arid/semiarid southwestern United States: Implications for probable maximum precipitation estimates. *J. Geophys. Res. Atmos.*, **123**, 1638–1656, https://doi.org/10.1002/2017JD027850.